Estimating transient crater size using the crustal annular bulge: Insights from numerical modeling of lunar basin-scale impacts

R. W. K. Potter,[1,2] D. A. Kring,[1] G. S. Collins,[2] W. S. Kiefer,[1] and P. J. McGovern[1]

Received 6 July 2012; revised 16 August 2012; accepted 21 August 2012; published 27 September 2012.

[1] The transient crater is an important impact cratering concept. Its volume and diameter can be used to predict impact energy and momentum, impact melt volume, and maximum depth and volume of ejected material. Transient crater sizes are often estimated using scaling laws based on final crater rim diameters. However, crater rim estimates, especially for lunar basins, can be controversial. Here, we use numerical modeling of lunar basin-scale impacts to produce a new, alternative method for estimating transient crater radius using the annular bulge of crust observed beneath most lunar basins. Using target thermal conditions appropriate for the lunar Imbrian and Nectarian periods, we find this relationship to be dependent on lunar crust and upper mantle temperatures. This result is potentially important when analyzing lunar basin subsurface structures inferred from the GRAIL mission. **Citation:** Potter, R. W. K., D. A. Kring, G. S. Collins, W. S. Kiefer, and P. J. McGovern (2012), Estimating transient crater size using the crustal annular bulge: Insights from numerical modeling of lunar basin-scale impacts, *Geophys. Res. Lett.*, *39*, L18203, doi:10.1029/2012GL052981.

1. Introduction

[2] The transient crater, an ephemeral form of the evolving crater marking the transition between excavation and collapse, is an important concept in impact cratering. Numerical and laboratory experiments have shown, for small craters, that transient crater volume and diameter can be used to predict, with reasonable accuracy, impact energy and momentum [*Holsapple*, 1982; *Schmidt and Housen*, 1987], impact melt volume [*Cintala and Grieve*, 1998], and maximum depth and volume of ejected material. Using field and remote observations of, respectively, terrestrial and lunar complex craters, scaling laws have been developed to estimate transient crater size based on observed crater rim diameters [e.g., *Croft*, 1985; *Holsapple*, 1993]. However, distinguishing the crater rim and therefore crater size, especially for large multi-ringed impact basins, is not trivial. Some basins have multiple crater rim estimates and this can lead to potentially significant errors in transient crater size estimates. The suitability of using scaling laws, based on observations of relatively small complex craters (where the structural relationship between the final and transient crater is clear), to infer transient crater radii from basin-scale features whose genetic link to the transient crater is less clear, is also questionable.

[3] An alternative way to estimate the transient crater radii of large lunar basins may be to use characteristic crustal thickness patterns observed under basins. Crustal thickness profiles, inferred from gravity and topography data, across the majority of large lunar basins show a relative thinning of crust beneath the basin center, surrounded by an annulus of relatively thickened crust (Figure 1) [*Wieczorek and Phillips*, 1999; *Hikida and Wieczorek*, 2007]. Crustal thickening is a result of crater excavation and collapse: overturn of crater-ejected material on to the target surface and inward collapse driven by the subsequent increase in overburden on the lithosphere [*Andrews-Hanna and Stewart*, 2011]. Here we propose that the radius of this crustal annulus (r_{ca}; measured at its greatest thickness - the bulge) is directly related to the transient crater radius (r_{tc}). We perform over two dozen lunar basin-forming numerical simulations to determine a scaling relationship between r_{ca} and r_{tc}. These simulations use target thermal conditions suitable for the latter stages of the lunar basin-forming epoch ~4 Ga. We find that the relationship between r_{ca} and r_{tc} is dependent on the thermal state of the lunar crust and upper mantle. Our relationship provides an independent estimate of transient crater radius and may aid analysis of GRAIL-inferred lunar basin crustal structures.

2. Methods

[4] We used the 2D iSALE hydrocode [*Amsden et al.*, 1980; *Collins et al.*, 2004; *Wünnemann et al.*, 2006], previously used to model large-scale impacts such as Chicxulub [*Collins et al.*, 2008] and South Pole-Aitken [*Potter et al.*, 2012], to model vertical (90°) lunar basin-forming impacts. A 3D hydrocode could be used to model oblique (<90°) impacts, but it would carry a high computational cost and cannot compete with the higher resolution capabilities of 2D models. The 2D models should also produce the correct azimuthally averaged behavior of crater formation for moderately oblique (c. 45°) impacts.

[5] An infinite half-space target was divided into crustal and mantle layers, the former of which was 40–60 km thick, based on gravity-derived lunar basin structures [*Wieczorek and Phillips*, 1999; *Hikida and Wieczorek*, 2007]. A Tillotson equation of state for gabbroic anorthosite [*Ahrens and O'Keefe*, 1977] and an ANEOS equation of state for dunite [*Benz et al.*, 1989] were used to represent the crustal and mantle responses, respectively, to both thermodynamic changes and compressibility; an ANEOS equation of state for dunite was also used for the impactor. Temperature was

[1]Center for Lunar Science and Exploration, Lunar and Planetary Institute, Houston, Texas, USA.
[2]Department of Earth Science and Engineering, Imperial College London, London, UK.

Corresponding author: R. W. K. Potter, Center for Lunar Science and Exploration, Lunar and Planetary Institute, Houston, TX 77058, USA. (potter@lpi.usra.edu)

©2012. American Geophysical Union. All Rights Reserved.
0094-8276/12/2012GL052981

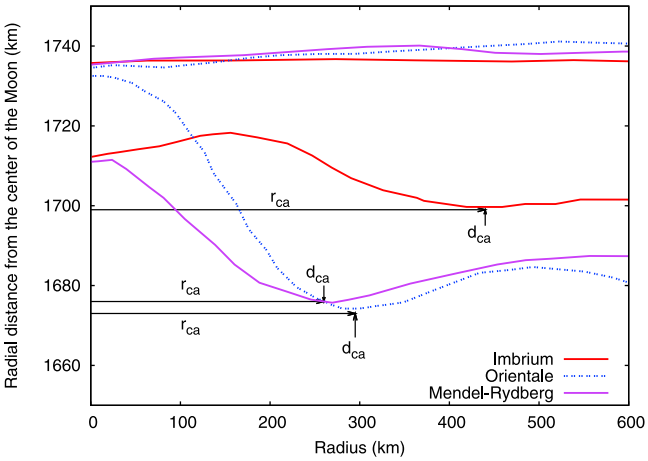

Figure 1. Gravity-derived crustal profiles for three lunar basins (data from *Hikida and Wieczorek* [2007]) showing the annular bulge of crustal material. r_{ca} is the radial distance of the crustal annulus from the basin center, measured at its thickest point (d_{ca}).

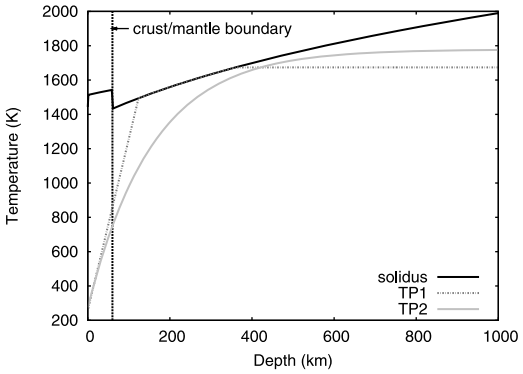

Figure 2. Target thermal profiles (TP1 and TP2) assuming a 60 km thick crust.

computed from internal energy in the Tillotson equation of state using the methodology described by *Ivanov et al.* [2002]. The low pressure gabbroic anorthosite phase was chosen over the high pressure phase as its parameters are more suited to describing the lunar crust. However, the low pressure phase equation of state will underestimate the temperature of gabbroic anorthosite in regions experiencing shock pressures between 15 GPa (the onset of the phase transition) and 100 GPa (the critical shock pressure for incipient melting of the low pressure phase [*Ahrens and O'Keefe*, 1977]). This will mostly affect hot crustal material around the basin center. Shock pressures experienced in the crust near the annular bulge, the region of importance in this work, are less than 10 GPa and therefore modeled in an appropriate manner by the low pressure gabbroic anorthosite phase. Material strength was accounted for using the strength model described by *Collins et al.* [2004] and a damage model described by *Ivanov et al.* [2010]. Crustal strength parameters were calculated from experimental gabbro strength [*Stesky et al.*, 1974; *Shimada et al.*, 1983] and melting [*Azmon*, 1967] data. Mantle strength parameters were calculated from experimental dunite and peridotite strength [*Shimada et al.*, 1983; *Ismail and Murrell*, 1990] data with curves for melt temperature as a function of pressure taken from *Davison et al.* [2010].

[6] Geological materials lose strength as their temperature increases, with all shear strength lost upon melting. However, the assumption of zero shear resistance at temperatures above the solidus is an oversimplification as super-solidus material will contain a mixture of melt, and hot and cold clasts, with the clasts providing some resistance to shear. To take this into account a partial melt viscosity of 10^{10} Pa · s was applied to super-solidus material [see *Potter*, 2012]. This acts as a useful first approximation as the rheology and behavior of impact-induced molten material is likely to be more complicated [*Stewart*, 2011].

[7] Acoustic fluidization [*Melosh*, 1979; *Melosh and Ivanov*, 1999], which is invoked to explain the collapse of complex craters and the formation of peaks and rings, is implemented in this work via the block model [*Melosh and Ivanov*, 1999; *Wünnemann and Ivanov*, 2003]. Block model parameters for lunar craters were chosen using the scaling relations of *Wünnemann and Ivanov* [2003] and constrained by models that reproduce the subsurface structure of the Chicxulub impact crater [*Collins et al.*, 2008]. For a list of model input parameters see Table S1 in the auxiliary material.[1]

[8] To simulate lunar basin-forming events up to approximately the size of Imbrium (~1200 km diameter), impactor diameter was varied between 40 and 120 km with impact velocities of 10 and 15 km/s. Cell size (varying between 1–3 km) was adjusted as a function of impactor radius to keep a constant number (20) of cells across the impactor radius providing a reasonable trade-off between computation time and resolution errors (Table S2 in the auxiliary material). Consequently, computation time increased as impactor (and cell) size decreased. Vapor production during impact was not important here so material with a density <300 kg/m^3 was removed from calculations (a mass equivalent to ~1% of the mass excavated/displaced by the transient crater) to expedite computation time. A spatially constant gravitational acceleration of 1.62 m/s^2 was used in all simulations. Impacts were modeled up to 3 hours after initial impact. The transient crater (measured at the pre-impact surface) was defined as forming once the transient cavity reached its greatest volume. This is similar to the approach of *Elbeshausen et al.* [2009] and provides a robust and easily defined estimate of transient crater size for basin-scale impacts.

[9] Thermal conditions during the latter stages of the lunar basin-forming epoch can be roughly constrained by the onset of mare volcanism, which began prior to the end of the basin-forming epoch ~4 Ga [*Hiesinger et al.*, 2011]. Partial melting at depths between 100–400 km in the mantle has been suggested as the mare basalt source region [*Heiken et al.*, 1991]. In this work, we used two target thermal profiles (Figure 2) consistent with that constraint. Thermal profile 1 (TP1), from *Potter et al.* [2012], has three components: a crustal and upper mantle thermal gradient of 10 K/km; mantle temperatures at the solidus between 150–350 km; and a deep (800 km) mantle temperature of 1670 K. The second thermal profile (TP2), from *Spohn et al.* [2001], has the same near-surface crustal gradient of 10 K/km;

[1]Auxiliary materials are available in the HTML. doi:10.1029/2012GL052981.

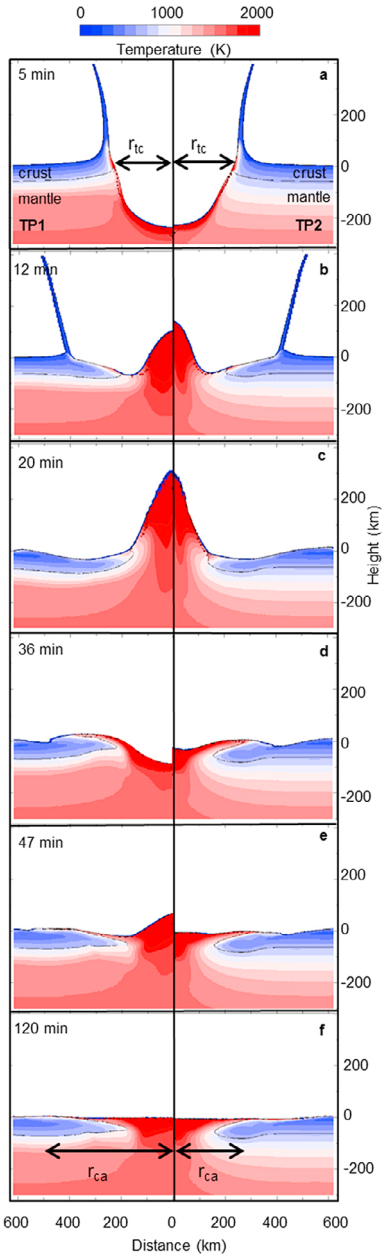

Figure 3. Basin formation timesteps for identical impact energies (impactor diameter 80 km; impact velocity 15 km/s) into (left) TP1 and (right) TP2. See text for discussion.

mantle temperatures that approach (though never reach) the solidus between 300 and 500 km; and a deep mantle temperature of 1770 K.

3. Results

[10] Figure 3 illustrates the formation of the annulus of thickened crust in the two different thermal profiles (TP1 and TP2) for identical impact energies (impactor diameter 80 km; impact velocity 15 km/s, both into a 60 km thick crust). Upon formation of the transient crater (Figure 3a), impact energy can no longer overcome gravity and the crater collapses, resulting in the uplift of material from the crater floor above the pre-impact target surface forming a central peak, as the ejecta curtain is draped over the target surface (Figures 3b and 3c). The peak eventually collapses back into the target (Figure 3d), with additional uplift and collapse phases possibly taking place (Figure 3e). Eventually the energy dissipates and the basin formation process is complete (Figure 3f). During central peak collapse (Figures 3c–3e) the relatively warmer and weaker lower crust and upper mantle of TP1 acts in a more ductile fashion than that of TP2, resulting in the movement of crustal material away from the basin center. In the case of the cooler, stronger TP2, the lower crust acts in a more rigid manner, with material from the collapsing central peak draping over the stronger crust creating a thicker and more prominent crustal annulus bulge closer to the basin center (see Figure S1 and Table S3 in the auxiliary material). The radius of the crustal annulus, r_{ca} (measured at its greatest thickness), is therefore greater for the impact into TP1 (486 km) than the impact into TP2 (263 km), despite their near-identical transient crater radii (r_{tc}) (TP1: 227 km, TP2: 223 km). The relationship between r_{tc} and r_{ca} and the effect of target thermal state for all simulations is shown in Figure 4. These data include impacts into targets with 40 and 60 km thick crusts, a suitable range for lunar basin pre-impact crustal thicknesses. These results suggest, for this crustal range and these thermal profiles, that crustal thickness does not have a strong effect on the relationship between transient crater radius and crustal annulus radius. For impacts into a Moon with TP1 the relationship is best approximated by the equation:

$$r_{tc} = 5.12 r_{ca}^{0.62} \quad (1)$$

For impacts with TP2 the relationship is best approximated by the equation:

$$r_{tc} = 4.22 r_{ca}^{0.72} \quad (2)$$

4. Discussion

[11] The simulations reveal that the basin-forming process is sensitive to the Moon's thermal state at the time of impact. In general, for the same impact energy, the crust thickens less, and more gradually, with radial distance, reaching a maximum crustal thickness further from the crater center if the upper mantle is warmer/weaker. In the two thermal states investigated here, material in the crustal annulus and

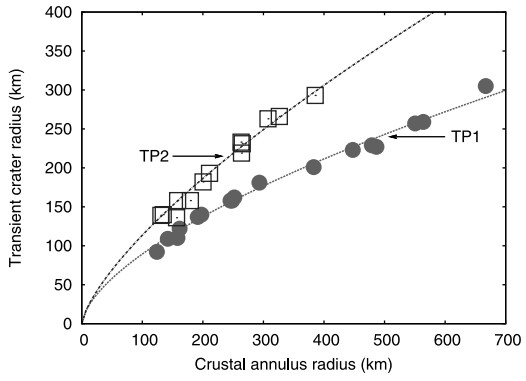

Figure 4. Transient crater radius and crustal annulus radius for simulated lunar basin-scale impacts using thermal profiles 1 (TP1: circles) and 2 (TP2: squares) fit by the least-squares method.

Table 1. Transient Crater Radius (r_{tc}) and Crustal Annulus Thickness (d_{ca}) Estimates[a]

Basin	r_r[b] (km)	r_{ca}[c] (km)	r_{tc}[f] (km)	r_{tc}[d] (km)	r_{tc}[e] (km) TP1	r_{tc}[e] (km) TP2	d_{ca}[c] (km)	d_{ca}[e] (km) TP1	d_{ca}[e] (km) TP2
Orientale	465	298	255	199	176	248	64	64	80
Imbrium	580	440	307	372	249	369	37	53	79
Serenitatis	460	414	252	329	216	314	50	48	73.5

[a]For further information about d_{ca}, see Figure S1 and Table S3 in the auxiliary material.
[b]Crater rim radius. Used by *Croft* [1985] to calculate r_{tc}.
[c]Calculated from *Hikida and Wieczorek* [2007].
[d]*Wieczorek and Phillips* [1999].
[e]This study.
[f]*Croft* [1985].

surrounding regions was relatively cool post-impact and no crustal relaxation was observed in the initial few hours after impact (the duration of the simulations). The calculated dimensions should therefore be a fair representation of structures in Imbrian and Nectarian aged lunar basins, which appear to show no significant relaxation [*Wieczorek and Phillips*, 1999; *Hikida and Wieczorek*, 2007]. We note, however, that older pre-Nectarian basins tend to lack a thinned crust and a prominent annular bulge [*Hikida and Wieczorek*, 2007]. *Bratt et al.* [1985] suggest this is primarily due to greater ductile flow rates in the crust during the earlier period of lunar basin formation when crustal temperatures were higher than those in the later periods.

[12] In our simulations, far more crustal material was removed from the basin centers than that suggested by gravity data [*Wieczorek and Phillips*, 1999; *Hikida and Wieczorek*, 2007]. The simulated basin centers were filled with a mixture of super-solidus, (partially and completely) molten crustal and mantle material, in agreement with numerical modeling of other (although larger) lunar basin-scale impact events [e.g., *Ivanov et al.*, 2010]. It is possible that, over time, this molten material could cool, crystallize and differentiate into a new crustal layer [*Morrison*, 1998], explaining differences in central basin structure between the simulations (basin structure a few hours after impact) and the gravity data (basin structure billions of years after impact).

[13] Interestingly, the relatively high target temperatures at the end of the lunar basin-forming epoch also appear to mitigate the role of acoustic fluidization during the uplift and subsequent collapse of the central peak. Acoustic fluidization was conceived to explain how impact rock debris can behave in a fluid-like manner on a timescale suitable for crater collapse through the reduction of overburden pressure during crater formation. However, in the simulations presented here, material behaved in a fluid-like manner primarily because the initially hot targets are weak by virtue of thermal softening.

[14] By applying Equations 1 and 2 to three late Nectarian/Imbrian basins (Table 1), we find our scaling laws for TP1 and TP2 generally predict smaller and larger r_{tc}, respectively, compared to *Croft* [1985] and *Wieczorek and Phillips* [1999]. *Croft* [1985] estimated r_{tc} by reconstructing terraces of terrestrial and lunar complex craters and relating this to the crater rim (see their equation 9). Transient crater estimations using this technique are therefore an extrapolation of trends from far smaller craters. *Wieczorek and Phillips* [1999] estimated r_{tc} by reconstructing the excavation cavity of lunar basins based on their gravity-derived crustal structures. However, they do not take into account any lateral movement of the crust during basin formation and do not consider any new crust being formed from the melt pool. Our estimates for the maximum thickness of the crustal annulus, d_{ca}, for these three basins are, in general, greater than those suggested by gravity data. Impacts into TP1 produce a lower d_{ca}, closer to the observed value, than those into TP2 because of TP1's warmer and more ductile crust. This might be because of our assumed pre-impact crustal thicknesses; if the actual pre-impact crust was thinner than our estimates, the maximum crustal thickness would be correspondingly lower. Our scaling laws emphasize the important effect of the pre-impact thermal state of the Moon and its consequences for impact cratering processes. By implication, the relationship between transient crater dimensions and impact-induced structures produced in planetary lithospheres may differ between planets.

[15] The effect of the Moon's thermal state is also illustrated by comparing our calculations for Imbrium and Orientale. Calculated r_{tc} values for an Orientale-size impact into TP2 and an Imbrium-size impact into TP1 are nearly identical (Table 1: 249 km and 248 km, respectively). If lunar thermal conditions at two different times or locations were comparable to our thermal states, both basins could have been produced by the same sized impactor (for a given impact velocity), despite their different r_r and r_{ca}. As the youngest basin, Orientale is likely to have impacted into a cooler Moon relative to any other basin. Imbrium is also young, however it impacted into the Procellarum KREEP Terrane, a region of heat producing elements and higher-than-average heat flow. Gravity data shows Orientale has a more prominent crustal annulus bulge compared to Imbrium which has a more gradual increase in crustal thickness and a less distinct annular bulge (see Figure 1). Our simulations show crustal thickness increases more gradually if the upper mantle is warmer/weaker. The relative differences in crustal structure between Imbrium and Orientale might therefore be explained by virtue of different thermal conditions during their formation.

5. Conclusions

[16] We propose a new, alternative method for estimating transient crater size using a relationship between the radius of the crustal annulus (measured at its greatest thickness) and the transient crater radius based on numerical models of lunar basin-scale impacts. The simulations show initial target temperature has a large effect on transient crater collapse and therefore impact basin structure; impacts with identical energies (similar size transient craters) produce very different post-impact crustal structures. This effect of initial target temperature should be considered when estimating transient

crater sizes and could therefore be important when analyzing lunar basin structures inferred from GRAIL.

[17] **Acknowledgments.** We thank Boris Ivanov, Jay Melosh, Kai Wünnemann and Dirk Elbeshausen for their work developing iSALE. We also thank Boris Ivanov and Jay Melosh for their thoughtful reviews. RWKP was partly funded by STFC grant ST/G002452/1, GSC was funded by NERC grant NE/E013589/1. Partial support was provided by NASA Lunar Science Institute contract NNA09DB33A (PI David A. Kring).

[18] The Editor thanks Boris Ivanov and Jay Melosh for assisting in the evaluation of this paper.

References

Ahrens, T. J., and J. D. O'Keefe (1977), Equations of state and impact-induced shock-wave attenuation on the moon, in *Impact and Explosion Cratering*, edited by D. J. Roddy et al., pp. 639–656, Pergamon, New York.

Amsden, A. A., H. M. Ruppel, and C. W. Hirt (1980), SALE: A Simplified ALE computer program for fluid flow at all speeds, *LANL Rep. LA-8095*, 101 pp., Los Alamos Natl. Lab., Los Alamos, N. M.

Andrews-Hanna, J. C., and S. T. Stewart (2011), The crustal structure of Orientale and implications for basin formation, *Lunar Planet. Sci. Conf.*, *42nd*, Abstract 2194.

Azmon, E. (1967), The melting of gabbro up to 45 kilobars, *NSL 67–224*, 16 pp., NASA, Washington, D. C.

Benz, W., A. G. W. Cameron, and H. J. Melosh (1989), The origin of the Moon and the single-impact hypothesis III, *Icarus*, *81*, 113–131, doi:10.1016/0019-1035(89)90129-2.

Bratt, S. R., S. C. Solomon, and J. W. Head (1985), The evolution of impact basins: Cooling, subsidence, and thermal stress, *J. Geophys. Res.*, *90*, 12,415–12,433, doi:10.1029/JB090iB14p12415.

Cintala, M. J., and R. A. F. Grieve (1998), Scaling impact melting and crater dimensions: Implications for the lunar cratering record, *Meteorit. Planet. Sci.*, *33*, 889–912, doi:10.1111/j.1945-5100.1998.tb01695.x.

Collins, G. S., H. J. Melosh, and B. A. Ivanov (2004), Modeling damage and deformation in impact simulations, *Meteorit. Planet. Sci.*, *39*, 217–231, doi:10.1111/j.1945-5100.2004.tb00337.x.

Collins, G. S., J. Morgan, P. Barton, G. L. Christeson, S. Gulick, J. Urrutia, M. Warner, and K. Wünnemann (2008), Dynamic modeling suggests terrace zone asymmetry in the Chicxulub crater is caused by target heterogeneity, *Earth Planet. Sci. Lett.*, *270*, 221–230, doi:10.1016/j.epsl.2008.03.032.

Croft, S. K. (1985), Scaling laws of complex craters, *Proc. Lunar Planet. Sci. Conf.*, *16th*, C828–C842.

Davison, T. M., G. S. Collins, and F. J. Ciesla (2010), Numerical modeling of heating in porous planetesimal collisions, *Icarus*, *208*, 468–481, doi:10.1016/j.icarus.2010.01.034.

Elbeshausen, D., K. Wünnemann, and G. S. Collins (2009), Scaling of oblique impacts in frictional targets: Implications for crater size and formation mechanisms, *Icarus*, *204*, 716–731, doi:10.1016/j.icarus.2009.07.018.

Heiken, G. H., D. T. Vaniman, and B. M. French (1991), *Lunar Sourcebook: A User's Guide to the Moon*, 736 pp., Cambridge Univ. Press, New York.

Hiesinger, H., J. W. Head, U. Wolf, R. Jaumann, and G. Neukum (2011), Ages and stratigraphy of lunar mare basalts: A synthesis, *Geol. Soc. Am. Spec. Pap.*, *477*, 1–51.

Hikida, H., and M. A. Wieczorek (2007), Crustal thickness of the Moon: New constraints from gravity inversions using polyhedral shape models, *Icarus*, *192*, 150–166, doi:10.1016/j.icarus.2007.06.015.

Holsapple, K. A. (1982), A comparison of scaling laws for planetary impact cratering: Experiments, calculations and theory, *Lunar Planet. Sci. Conf.*, *13th* Abstract 1172.

Holsapple, K. A. (1993), The scaling of impact processes in planetary sciences, *Annu. Rev. Earth Planet. Sci.*, *21*, 333–373, doi:10.1146/annurev.ea.21.050193.002001.

Ismail, I. A. H., and S. A. F. Murrell (1990), The effect of confining pressure on stress-drop in compressive rock fracture, *Tectonophysics*, *175*, 237–248, doi:10.1016/0040-1951(90)90140-4.

Ivanov, B. A., F. Lagenhorst, A. Deutsch, and U. Hornamann (2002), How strong was impact-induced CO_2 degassing in the Creataceous-Tertiary event? Numerical modeling of shock recovery experiments, *Geol. Soc. Am. Spec. Pap.*, *356*, 587–594.

Ivanov, B. A., H. J. Melosh, and E. Pierazzo (2010), Basin-forming impacts: Reconnaissance modeling, *Geol. Soc. Am. Spec. Pap.*, *465*, 29–49.

Melosh, H. J. (1979), Acoustic fluidization: A new geologic process? *J. Geophys. Res.*, *84*, 7513–7520.

Melosh, H. J., and B. A. Ivanov (1999) Impact crater collapse, *Annu. Rev. Earth Planet. Sci.*, *27*, 385–415, doi:10.1146/annurev.earth.27.1.385.

Morrison, D. A. (1998), Did a thick South Pole-Aitken basin melt sheet differentiate to form cumulates?, *Lunar Planet. Sci. Conf.*, *29th*, Abstract 1657.

Potter, R. W. K. (2012), Numerical modelling of basin-scale impact crater formation, PhD thesis, Imp. Coll. London, London.

Potter, R. W. K., G. S. Collins, W. S. Kiefer, P. J. McGovern, and D. A. Kring (2012), Constraining the size of the South Pole-Aitken basin impact, *Icarus*, *220*, 730–743, doi:10.1016/j.icarus.2012.05.032.

Schmidt, R. M., and K. Housen (1987), Some recent advances in the scaling of impact and explosion cratering, *Int. J. Impact Eng.*, *5*, 543–560, doi:10.1016/0734-743X(87)90069-8.

Shimada, M., A. Cho, and H. Yukutake (1983), Fracture strength of dry silicate rocks at high confining pressures and activity of acoustic emission, *Tectonophysics*, *96*, 159–172, doi:10.1016/0040-1951(83)90248-2.

Spohn, T., W. Konrad, D. Breuer, and R. Ziethe (2001), The longevity of lunar volcanism: Implications of thermal evolution calculations with 2D and 3D mantle convection models, *Icarus*, *149*, 54–65, doi:10.1006/icar.2000.6514.

Stesky, R. M., W. F. Brace, D. K. Riley, and P. Y. Bobin (1974), Friction in faulted rock at high temperature and pressure, *Tectonophysics*, *23*, 177–203, doi:10.1016/0040-1951(74)90119-X.

Stewart, S. T. (2011), Impact basin formation: The mantle excavation paradox resolved, *Lunar Planet. Sci. Conf.*, *42nd*, Abstract 1633.

Wieczorek, M. A., and R. J. Phillips (1999), Lunar multiring basins and the cratering process, *Icarus*, *139*, 246–259, doi:10.1006/icar.1999.6102.

Wünnemann, K., and B. A. Ivanov (2003), Numerical modelling of the impact crater depth-diameter dependence in an acoustically fluidized target, *Planet. Space Sci.*, *51*, 831–845, doi:10.1016/j.pss.2003.08.001.

Wünnemann, K., G. S. Collins, and H. J. Melosh (2006), A strain-based porosity model for use in hydrocode simulations of impacts and implications for transient crater growth in porous targets, *Icarus*, *180*, 514–527, doi:/10.1016/j.icarus.2005.10.013.